Available online at www.sciencedirect.com
SCIENCE DIRECT®
Marine Geology 203 (2004) 177–184
MARINE GEOLOGY
INTERNATIONAL JOURNAL OF MARINE GEOLOGY, GEOCHEMISTRY AND GEOPHYSICS
www.elsevier.com/locate/margeo

Methane solubility in marine hydrate environments

M.K. Davie, O.Y. Zatsepina, B.A. Buffett *

Department of Earth and Ocean Sciences, University of British Columbia, Vancouver, BC, Canada V6T 1Z4

Received 17 October 2002; received in revised form 14 April 2003; accepted 9 September 2003

Abstract

Modeling of gas hydrate formation below the seafloor requires accurate estimates of the methane solubility in marine sediments. Although the methane solubility is relatively well-established, a practical method for calculating solubilities under marine conditions is currently unavailable in the literature. We present a method of predicting the solubility in a marine setting for a given water depth, seafloor temperature and geothermal gradient. In this method, pressure and temperature conditions at the base of the hydrate stability zone (HSZ) are determined by finding the intersection of the local P, T conditions with experimentally determined conditions for three-phase equilibrium between water, hydrate and free gas. Phase equilibrium calculations of Zatsepina and Buffett [Zatsepina, O.Y., Buffett, B.A. (1997) Geophys. Res. Lett. 24, 1567–1570] are used to predict the methane solubility at the base of the HSZ, and simple parametric models are used to extend the solubility into the HSZ. The depth dependence of the methane solubility is computed at four known hydrate locations to provide constraints on the primary source of methane at these locales.

Keywords: gas hydrate; methane; solubility; phase equilibrium; modeling

1. Introduction

Marine hydrate is restricted to locations where the necessary pressure and temperature conditions are met and where the abundance of methane is sufficient to exceed the local solubility (Kvenvolden, 1988). Although pressure and temperature conditions are satisfied throughout most of the world's oceans, hydrate occurrences are generally restricted to continental margins where conversion of high inputs of organic carbon or focusing of methane bearing fluids supply the methane required for hydrate formation. The equilibrium methane concentration (or solubility) is important because it determines the minimum methane concentration needed for hydrate stability. Once hydrate forms in marine sediments the concentration of methane in the pore water is fixed by the equilibrium concentration. As a result, changes in solubility with depth below the seafloor control the diffusive loss of methane from locations where the hydrate is present. In fact, numerical models for the formation of hydrate show that the shape of the solubility profile has a strong influence on the methane supply needed to form hydrate, as well the resulting vertical distribution of hydrate in the sediments (Davie and Buffett, 2001). In addition,

* Corresponding author.
E-mail addresses: davie@geop.ubc.ca (M.K. Davie), olga@geop.ubc.ca (O.Y. Zatsepina), buffett@eos.ubc.ca (B.A. Buffett).

0025-3227/03/$ – see front matter © 2003 Elsevier B.V. All rights reserved.
doi:10.1016/S0025-3227(03)00331-1

the methane solubility is used to infer hydrate volumes from direct measurements of in situ methane quantities (Dickens et al., 1997).

The base of the hydrate stability zone (HSZ) coincides with the depth where the local pressure and temperature conditions match the conditions for three-phase equilibrium between water, hydrate and free gas (Fig. 1). Only two phases are expected to coexist above and below the base of the HSZ. The abundance of water in marine settings ensures that water coexists with hydrate inside the HSZ, whereas water and free gas are the stable phases at depths below the HSZ (Duan et al., 1992). Several previous studies have obtained estimates of the methane solubility at conditions appropriate for natural hydrate settings. The experimental study of Culberson and McKetta (1951) measured the solubility of methane at conditions appropriate for the region below the HSZ, while Handa (1990) theoretically examined the influence of pressure on methane solubility inside the HSZ. Applying these results to marine hydrate occurences indicates that the solubility within the HSZ decreases towards the seafloor (Rempel and Buffett, 1997). A subsequent study by Zatsepina and Buffett (1997) used thermodynamic calculations to predict the methane solubility within and below the HSZ. This work was later extended to include the influence of salts (Zatsepina and Buffett, 1998). More recent experimental work of Yang et al. (2001) and Servio and Englezos (2002) confirm the decrease in methane solubility towards the seafloor inside the HSZ.

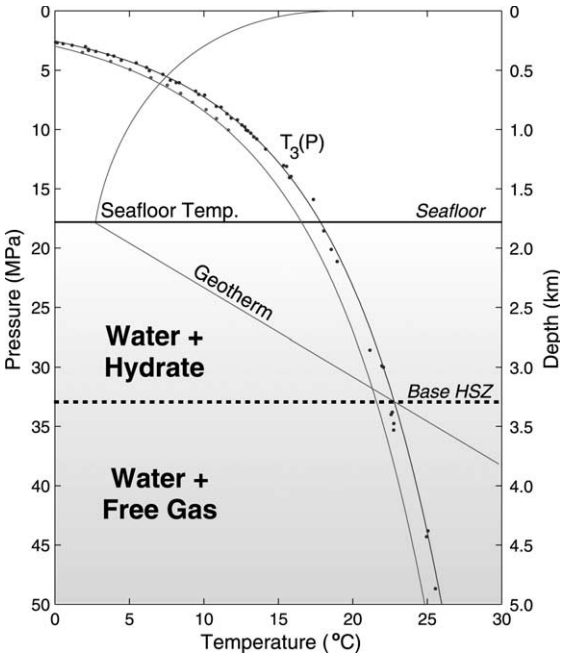

Fig. 1. Schematic profile of the HSZ in marine sediments. The intersection of the local geotherm with the temperature T_3 for three-phase equilibrium of the water-hydrate-free gas system defines the base of the HSZ. Experimental data for three-phase equilibrium of pure (Sloan, 1990) and salt water (Dickens and Quinby-Hunt, 1994) are shown as dots, while the empirical fit of Brown and Bangs (1995) are shown as solid lines. Salt water reduces the three-phase equilibrium temperature $T_3(P)$ by $\sim$1.5°C.

Although the solubility of methane is now relatively well-established, a practical method of predicting the solubility under marine conditions is not presently available in the literature. In this paper, we present a method of predicting the solubility in a marine setting for a given the water depth, seafloor temperature and geothermal gradient. The base of the HSZ is defined by the temperature $T_3(P)$ for three-phase equilibrium between water, hydrate and free gas. Locating the base of the HSZ is done by finding the intersection of the local geotherm with the phase boundary at $T_3(P)$. We then evaluate the methane solubility at the conditions of three-phase equilibrium using the phase equilibrium predictions of Zatsepina and Buffett (1997). The solubility is then extended into the region within and below the HSZ using simple parametric models that have been fit to the calculated solubilities.

2. HSZ

The phase boundary for methane hydrate has been determined experimentally for both pure water (as reviewed by Sloan (1990)) and seawater (Dickens and Quinby-Hunt, 1994). Intersection of the local geotherm with $T_3(P)$ defined the base of the HSZ (Fig. 1). Hydrate decomposes at greater depths, releasing large volumes of methane. This methane is incorporated into free gas, causing a large P-wave velocity contrast which is commonly observed as a bottom simulating reflector on ma-

rine seismic profiles (Stoll et al., 1971; Shipley et al., 1979). Good agreement is often found between experimental estimates of $T_3(P)$ and the observed P, T conditions at the base of the HSZ from hydrate locations (Fig. 2). Pressure in marine settings is defined by the water depth while temperature is defined by both the seafloor temperature and the local geothermal gradient. By providing these parameters at a specific site, an estimate of the depth of the base of the HSZ can be made.

The depth below the seafloor, z, is converted to a corresponding pressure by assuming a hydrostatic relationship

$$P(z) = \rho_f g(H + z) \quad (1)$$

where ρ_f is the density of seawater (1035 kg/m^3), g is the gravitational acceleration (9.8 m/s^2), and H is the water depth. More accurate approximations for converting depth to pressure are discussed by Peltzer and Brewer (2001). Temperature in the sediments is expressed as a linear function of depth,

$$T(z) = T(0) + Gz \quad (2)$$

where $T(0)$ is the seafloor temperature and G is the local geothermal gradient. The theoretical base of the HSZ can be established by incrementally increasing z from the seafloor until $T(z)$ intersects $T_3(P)$. At each z, $T(z)$ is calculated using Eq. 2 and $P(z)$ is evaluated using Eq. 1. The value of $T_3(P)$ is determined using either an empirical formula (Brown and Bangs, 1995) or by interpolating experimental measurements (Sloan, 1990; Dickens and Quinby-Hunt, 1994). When $T(z) < T_3(P)$, the depth is incremented and the calculation is repeated until $T(z) = T_3(P)$. The final $T(z)$ and P defines the base of the HSZ.

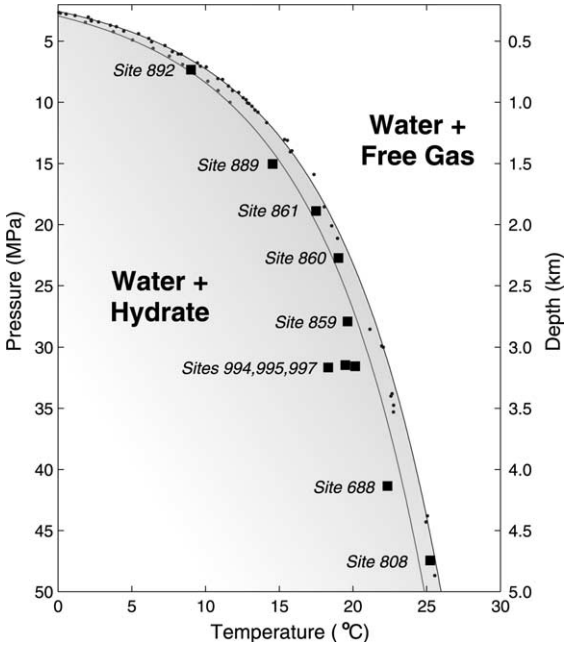

Fig. 2. Comparison of P, T conditions at the base of the HSZ in natural hydrate settings (solid squares) with the three-phase equilibrium pressure and temperature (i.e. T_3, P_3) of the water-hydrate-free gas system. $T_3(P)$ is shown for the pure water (blue) and salt water (red). Relatively good agreement is observed between the pressure–temperature conditions in natural settings and experimental three-phase pressure–temperature.

3. Methane solubility profile

A practical method for determining methane solubility below the seafloor relies on simple parametric equations to accurately reproduce the solubilities obtained from thermodynamic calculations or experiments. We use the thermodynamic predictions of Zatsepina and Buffett (1997) to determine the methane solubility in two steps. We first approximate the solubility at the conditions of three-phase equilibrium and then extend this solubility into the HSZ using simple parametric equations. The region below the HSZ is handled separately.

Fig. 3 shows the thermodynamic predictions of methane solubility in pure water as a function of temperature for three values of pressure. The peak in the solubilities occurs at $T_3(P)$, which coincides with the base of the HSZ. The solubility at $T_3(P)$ can be represented as a linear function of temperature and pressure according to

$$C_3(T,P) = C_3(T_o,P_o) + \frac{\partial C_3}{\partial T}(T - T_o) + \frac{\partial C_3}{\partial P}(P - P_o), \quad (3)$$

where $C_3(T_o,P_o)$ is the solubility in mM at a suitable reference temperature T_o and pressure P_o.

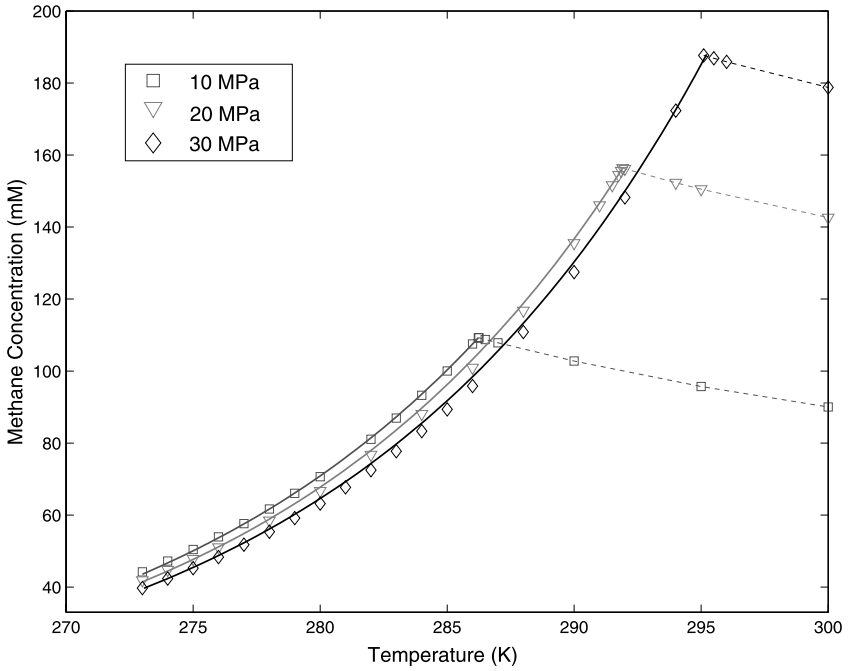

Fig. 3. Solubility of methane in pure water as a function of temperature at fixed pressures of 10 MPa (squares), 20 MPa (circles) and 30 MPa (crosses) calculated by Zatsepina and Buffett (1997) (from Table 1). The peak in the solubilities occurs at $T_3(P)$, which coicides with the base of the HSZ. Good agreement between the results of Zatsepina and Buffett (1997) and solubilities predicted according to 5 (solid lines) is observed at temperatures below $T_3(P)$ (dashed lines connect solubility data above $T_3(P)$).

The partial derivatives $\partial C_3/\partial T$ and $\partial C_3/\partial P$ are estimated by fitting Eq. 3 to the solubilities listed in Table 1. The resulting values are

$$\frac{\partial C_3}{\partial T} = 6.34 \text{ mM}/^{\circ}\text{K} \quad \frac{\partial C_3}{\partial P} = 1.11 \text{ mM/MPa}, \tag{4}$$

when we adopt a reference solubility of $C_3(T_o,P_o) = 156.36$ mM at $T_o = 292$ K and $P_o = 20$ MPa. Using Eq. 3 with the reference solubility and constants in Eq. 4 gives an accurate estimate of solubility at the base of the HSZ.

At temperatures lower than $T_3(P)$ (within the HSZ), water and hydrate are the stable phases. Because the compressibility of both water and hydrate is small, the solubility profile is relatively insensitive to pressure. In fact, the solubility can be accurately represented within the HSZ as an exponential function of temperature

$$c_{eq}(T) = C_3(T_3, P)\exp\left(\frac{T-T_3}{\alpha}\right) \tag{5}$$

where $C_3(T_3,P)$ is evaluated using Eq. 3 at conditions coinciding with the base of the HSZ and $\alpha = 14.4$°C is determined by fitting Eq. 5 to the theoretical values listed in Table 1. We have written $c_{eq}(T)$ solely as a function of T because the pressure dependence of C_3 refers to the base of the HSZ and not the pressure inside the HSZ where $c_{eq}(T)$ is being evaluated. A graphical comparison of the theoretical solubilities and the predictions of Eq. 5 is shown in Fig. 3. The good agreement confirms the accuracy of the simple representation in Eq. 5.

At temperatures above $T_3(P)$, water and free gas are the stable phases. In this case, the solubility profile is a function of both the temperature and pressure because free gas is highly compressable. An increase in depth z causes an increase in both pressure and temperature according to Eq. 1 and Eq. 2. From Fig. 3, we see that increases in pressure and temperature affect the solubility below the HSZ in opposite ways. Increased pressure causes an increase in solubility, while an increase in temperature causes a decrease in solubility. At

Table 1
Solubility of methane in pure water as a function of temperature predicted by the thermodynamic calculations of Zatsepina and Buffett (1997) at fixed pressures of 10 MPa, 20 MPa and 30 MPa

$P = 10$ MPa		$P = 20$ MPa		$P = 30$ MPa	
Temp. (°K)	Conc. (mM)	Temp. (°K)	Conc. (mM)	Temp. (°K)	Conc. (mM)
273.00	44.21	273.00	41.88	273.00	39.71
274.00	47.21	274.00	47.76	274.00	42.36
275.00	50.43	275.00	47.81	275.00	45.25
276.00	53.93	276.00	51.06	276.00	48.33
277.00	57.63	278.00	58.50	277.00	51.77
278.00	61.68	280.00	66.70	278.00	55.39
279.00	66.02	282.00	76.74	279.00	59.15
280.00	70.67	284.00	88.10	280.00	63.19
282.00	81.03	286.00	100.94	281.00	67.68
283.00	86.94	288.00	116.79	282.00	72.48
284.00	93.26	290.00	135.54	283.00	77.75
285.00	100.00	291.00	146.04	284.00	83.29
286.00	107.51	291.50	151.63	285.00	89.35
286.23	109.26	291.75	154.46	286.00	95.83
286.25	109.23	291.85	155.63	288.00	110.84
286.50	108.76	291.91	156.36	290.00	127.50
287.00	107.85	292.00	156.19	292.00	148.24
290.00	102.79	294.00	152.32	294.00	172.33
295.00	95.72	295.00	150.51	295.10	187.68
300.00	90.03	300.00	142.62	295.50	186.88
				296.00	185.89
				300.00	178.79

conditions representative of natural hydrate settings, the changes in solubility with depth below the HSZ are small due to counter-acting effects of pressure and temperature (see fig. 3 of Zatsepina and Buffett (1997)). For many applications (e.g. numerical modeling) the solubility profile below the HSZ can be approximated by

$$c_{eq}(z) = c_{eq}(T_3). \tag{6}$$

More accurate approximations are obtained by interpolating between the values listed in Table 1, or by using the model of Duan et al. (1992).

The variations in methane solubility with depth can now be calculated at a marine setting using the water depth, seafloor temperature and geothermal gradient. The thermodynamic conditions (P,T) and depth at the base of the HSZ are determined iteratively using estimates for $T_3(P)$. The solubility at three-phase equilibrium is then calculated using Eq. 3 with the constants in Eq. 4. Finally, the solubilities in the two-phase regions are calculated using Eq. 5 within the HSZ and Eq. 6 below. The profile of solubility within the HSZ can be expressed as a function of depth by converting the temperature to depth according to Eq. 2.

4. Influence of salt

The presence of salts in seawater shifts the base of the HSZ zone to shallower depths and causes a small reduction in the solubility of methane (Handa, 1990). Estimates for the change in $T_3(P)$ have been given by Dickens and Quinby-Hunt (1994), and these results are incorporated into the empirical formula of Brown and Bangs (1995). Fig. 1 shows the predicted stability curve for a typical concentration of salts in seawater. Changes in methane solubility have been calculated by Zatsepina and Buffett (1998) using a 0.6-mol solution of NaCl in water as an approximation for seawater (the activity of water in a 0.6-mol solution of NaCl is comparable to that of seawater). Their calculation for C_3 indicates a linear dependence on the concentration of salt S, so we account for the influence of salt using

$$C_3(T,P,S) = (1-\beta S)C_3(T,P,0), \tag{7}$$

where $C_3(T,P,0)$ is calculated from Eq. 3 and $\beta = 0.1$ mol^{-1} is determined from the results of Zatsepina and Buffett (1998).

Changes in methane solubility within the HSZ have a more complicated dependence on S. Calculations for a 0.6-mol solution of NaCl predicts a reduction in the solubility, but most of this reduction relative to pure water occurs as S is increased from $S = 0$ to $S = 0.1$ mol (see fig. 5 of Zatsepina and Buffett (1998)). Further increases in S cause a very small increase in c_{eq}, although the rate of increase is so small that the overall reduction in c_{eq} (above $S = 0.1$ mol) is nearly independent of S. The temperature dependence of c_{eq} in seawater is accurately described by Eq. 5 within the HSZ, so the procedure described in the previous section for pure water is readily extended to account for the influence of salt. We first determine the base of the HSZ using the

stability curve for seawater. We then calculate the solubility at three-phase equilibrium using Eq. 7. We extend the solubility into the HSZ using Eq. 5. (A fit of Eq. 5 to the solubilities calculated in saltwater yields $\alpha = 14.5$, which is nearly identical to the value in pure water). Finally, we use Eq. 6 to determine the solubilities immediately below the stability zone.

5. Discussion

The solubility defines the minimum methane concentration needed to form hydrate. This concentration of methane must be established and maintained by conversion of organic matter in hydrate bearing sediments, so higher solubilities imply higher requirements for conversion of organic matter. Additional insight into the methane production can be obtained from the slope of the solubility profile within the HSZ. The slope of the solubility profile determines the rate of methane loss by diffusion from locations where hydrate is present. A comparable supply of methane is needed to maintain the hydrate volume. An examination of solubility profiles at specific hydrate locations allows us to speculate about the mechanism of methane supply which prevails at these sites. As an example, we consider four known hydrate locations: Site 997 on the Blake Ridge (Paull et al., 1996), Site 688 on the Peru Margin (Suess et al., 1988), Site 889 on the Cascadia Margin (Westbrook et al., 1994) and Site 860 on the Chile Triple Junction (Behrmann et al., 1992). Solubility profiles at each of these locations are calculated using the procedure outline in Section 4 (see Fig. 4).

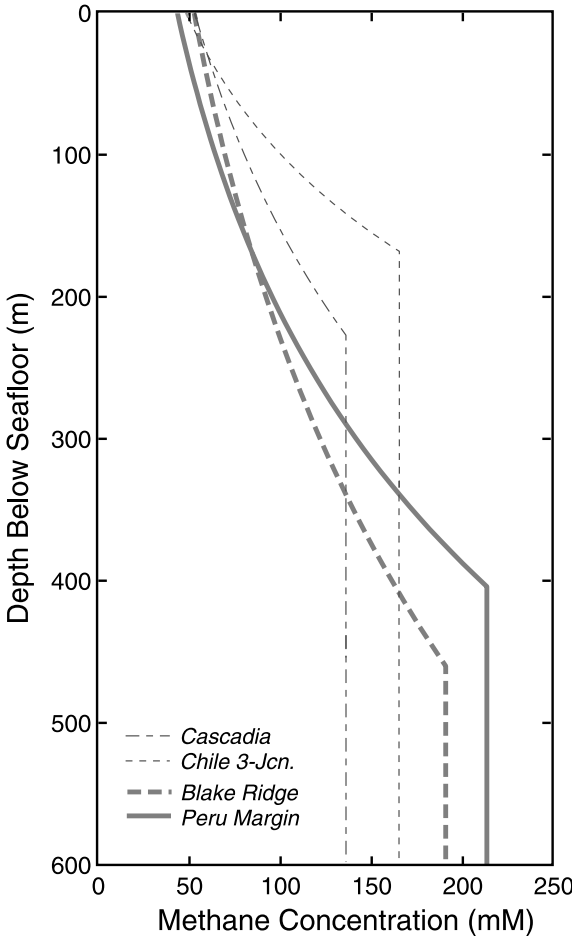

Fig. 4. Solubility profiles of four known hydrate locations. Pressure and temperature conditions at the Blake Ridge and Peruvian Margin result in thicker zones of hydrate stability and smaller slopes in the solubility profile within the HSZ (solid lines). On the other hand, the Cascadia Margin and Chile Triple Junction have thin HSZ's and a steeper slope of the solubility profile within the HSZ.

Qualitative interpretation of the mechanism of methane supply can be made by examining the solubility profiles. The pressure and temperature conditions at the Blake Ridge and Peruvian Margin result in thick zones of hydrate stability (450 and 400 mbsf respectively). As a result, the slopes of the solubility profiles (within the HSZ) at the Blake Ridge and Peruvian Margin are smaller than those of the other two sites (Fig. 4). This smaller slope reduces the loss of methane due to chemical diffusion within the depth interval where hydrate is present, and thereby reduces the rate of methane supply needed to maintain the hydrate. Lower rates of methane supply mean that less in situ conversion of total organic carbon (TOC) to sustain the hydrate (if this is the principal source of methane). Higher than average TOC at both the Blake Ridge and Peruvian Margin (1.5% and 3% respectively) make both sites more likely to accumulate hydrate through in situ conversion of organic material.

On the other hand, pressure and temperature conditions at both the Cascadia Margin and Chile Triple Junction yield thin zones of hydrate stability (~230 mbsf and 160 mbsf respectively). Consequently, the slope of solubility profiles (within the HSZ) are steeper at both the Cascadia Margin and Chile Triple Junction (Fig. 4). As a result, methane is lost more rapidly from the hydrate zone, increasing the demand on the methane supply. However, low average TOC within the sediments at both the Cascadia Margin and Chile Triple Junction (<1% and <0.5% respectively) indicates that in situ biogenic conversion of organic carbon may not be sufficient to maintain hydrate at these sites. Such low TOC values argue for other sources of methane. Of course, it is possible that these occurrences formed at an earlier time when the average TOC was higher and are now disappearing due to the persistent loss of methane by diffusion through the pore water. However, focusing of deep methane sources is thought to be the primary mechanism of methane supply at the Cascadia Margin (Hyndman and Davis, 1992) and the Chile Triple Junction (Brown et al., 1996).

Locations of hydrate occurrence are controlled by the combination of the pressure and temperature conditions (which define the solubility profile) and an adequate supply of methane. In order to make better predictions of hydrate occurrence and global hydrate inventories, numerical models must account for the solubility and the methane supply. Recent numerical models of Davie and Buffett (2001) show that the conditions for hydrate formation cannot be defined simply by the TOC in the sediments or by a critical flux of methane due to fluid migration (Xu and Ruppel, 1999). The shape of the solubility profile and even the rate of sedimentation can also be important factors for determining whether hydrates form. Previous attempts to estimate the global abundance of hydrate based on estimates of TOC (Kvenvolden, 1988) or on satellite data of phytoplankton concentration as a proxy for TOC (Gornitz and Fung, 1994) do not account for site-dependent pressures and temperatures, which greatly influence the profile of methane solubility and thus the demands on the methane supply. Some improvements in the global estimate of hydrate volume might be obtained by adjusting the required TOC (or methane flux) to account for variations in the rate of methane loss due to diffusion, although more reliable results will require the use of site-dependent solubility profiles in numerical models.

6. Conclusions

We present a practical method of calculating the solubility profile within the HSZ in a marine setting. By providing the water depth, seafloor temperature and geothermal gradient at a specific location, we are able to calculate the pressure and temperature conditions at the base of the HSZ. The methane solubility is then calculated at the conditions of three-phase equilibrium using the phase equilibrium results of Zatsepina and Buffett (1997). Simple parametric models are used to extend the results into the regions above and below the HSZ.

The solubility profiles at four hydrate locations were examined to qualitatively interpret possible mechanisms of methane supply. It was found that sites with steep solubility profiles and low TOC (i.e. Cascadia Margin and Chile Triple Junction) favored the focusing of deep methane sources as the main mechanism of methane supply, while sites with a smaller slope of the solubility profile within the HSZ and higher TOC (Blake Ridge and Peruvian Margin) suggest that biogenic production of methane may be important at these locations.

References

Behrmann, J., Lewis, S., Musgrave, S., et al., 1992. Proceedings of the Ocean Drilling Program, Initial Results, Vol. 141. College Station, TX.

Brown, K.M., Bangs, N.L., 1995. Thermal regime of the Chile Triple Junction: Constraints provided by downhole temperature measurements and distribution of gas hydrate. In: Lewis, S.D., Behrmann, J.H. Musgrave, R.J., Cande, S.C. (Eds.), Proceedings of the Ocean Drilling Program, Scientific Results, Vol. 164. College Station, TX.

Brown, K.M., Bangs, N.L., Froelich, P.N., Kvenvolden, K.A., 1996. The nature, distribution, and origin of gas hydrate in

the Chile Triple Junction region. Earth Planet. Sci. Lett. 139, 471–483.

Culberson, L., McKetta, J., 1951. Phase equilibrium in hydrocarbon-water systems III: The solubility of methane in water at pressures to 10,000 psia. Petro. Trans. AIME 192, 223–226.

Davie, M.K., Buffett, B.A., 2001. A numerical model for the formation of gas hydrate below the seafloor. J. Geophys. Res. 106, 497–514.

Dickens, G.R., Paull, C.K., Wallace, P., Leg 164 Science Party, 1997. Direct measurement of in situ methane quantities in a large gas-hydrate reservoir. Nature 25, 259–262.

Dickens, G.R., Quinby-Hunt, M.S., 1994. Methane hydrate stability in seawater. Geophys. Res. Lett. 21, 2115–2118.

Duan, Z., Miller, N., Greenberg, J., Weare, J., 1992. The prediction of methane solubility in natural waters to high ionic strengths from 0 to 250 c and from 0 to 1600 bar. Geochim. Cosmochim. Acta 56, 1451–1460.

Gornitz, V., Fung, I., 1994. Potential distribution of methane hydrates in the world's oceans. Global Biogeochem. Cycles 8, 335–347.

Handa, Y.P., 1990. Effect of hydrostatic pressure and salinity on the stability of gas hydrates. J. Phys. Chem. 94, 2652–2657.

Hyndman, R.D., Davis, E.E., 1992. A mechnism for the formation of methane hydrate and seafloor bottom-simulating reflectors by vertical fluid expulsion. J. Geophys. Res. 97, 7025–7041.

Kvenvolden, K.A., 1988. Methane hydrate – A major reservoir of carbon in the shallow geosphere? Chem. Geol. 71, 41–51.

Paull, C.K., Matsumoto, R., Wallace, P.J., et al., 1996. Proceedings of the Ocean Drilling Program, Initial Results, Vol. 164. College Station, TX.

Peltzer, E.T., Brewer, P.G., 2001. Practical physical chemistry and empirical predictions of methane hydrate stability. In: Max, M. (Ed.), Natural Gas Hydrate in Oceanic and Permafrost Environments. Kluwer Academic Publishers, pp. 17–28.

Rempel, A., Buffett, B.A., 1997. Formation and accumulation of gas hydrate in porus media. J. Geophys. Res. 102, 10151–10164.

Servio, P., Englezos, P., 2002. Measurement of dissolved methane in water in equilibrium with its hydrate. J. Chem. Eng. Data 47, 87–90.

Shipley, T.H. et al., 1979. Seismic reflection evidence for the widespread occurrence of possible gas-hydrate horizons on continental slopes and rises. AAPG Bull. 63, 2204–2213.

Sloan, E.D., 1990. Clathrate Hydrates of Natural Gases. Marcel Dekker, New York.

Stoll, R., Ewing, J., Bryan, G., 1971. Anomalous wave velocity in sediments containing gas hydrates. J. Geophys. Res. 76, 2090–2094.

Suess, E., von Huene, R., Emeis, K., Bougois, J. et al., 1988. Proceedings of the Ocean Drilling Program, Initial Results, Vol. 112. College Station, TX.

Westbrook, G.K., Carson, B., Musgrave, R.J., et al., 1994. Proceedings of the Ocean Drilling Program, Initial Results, Vol. 146, (Pt1). College Station, TX.

Xu, W., Ruppel, C., 1999. Predicting the occurrence, distribution, and evolution of methane gas hydrate inporous marine sediments. J. Geophys. Res. 104 (B3), 5081–5095.

Yang, S.O., Cho, S.H., Lee, H., Lee, C.S., 2001. Measurement and prediction of phase equilibria for water+methane in hydrate forming conditions. Fluid Phase Equilib. 185, 53–63.

Zatsepina, O.Y., Buffett, B.A., 1997. Phase equilibrium of gas hydrate: Implications for the formation of hydrate in the deep sea floor. Geophys. Res. Lett. 24, 1567–1570.

Zatsepina, O.Y., Buffett, B.A., 1998. Conditions for the stability of gas hydrate in the seafloor. J. Geophys. Res. 103, 24127–24139.